Proceedings of the 17th Czech and Slovak Conference on Magnetism, Košice, Slovakia, June 3–7, 2019

Interlayer Dzyaloshinskii–Moriya Interactions in a Quasi-Two-Dimensional Spin 1/2 Antiferromagnet $Cu(en)(H_2O)_2SO_4$

J. Chovan[a,b,c], L. Lederová[d], A. Orendáčová[d,*], R. Tarasenko[d], V. Tkáč[d], M. Orendáč[d], D. Legut[a] and A. Feher[d]

[a]IT4Innovations National Supercomputing Center, VSB-Technical University of Ostrava, 17. listopadu 2172/15, CZ 708 33 Ostrava, Czech Republic

[b]Department of Physics, Matej Bel University, Tajovského 40, 974 01 Banská Bystrica, Slovakia

[c]International Clinical Research Center, St. Anne's University Hospital, Pekařská 53, 656 91 Brno, Czech Republic

[d]Institute of Physics, P.J. Šafárik University, Park Angelinum 9, 040 01 Košice, Slovakia

We present a theoretical study of magnetic interlayer exchange couplings in a quasi-two-dimensional quantum antiferromagnet $Cu(en)(H_2O)_2SO_4$ (en =$C_2H_8N_2$). We use symmetry arguments to construct the most general form of interlayer spin exchange interactions, and discuss the significance of individual terms. Particular attention is paid to the antisymmetric Dzyaloshinskii–Moriya spin anisotropy, allowed for the interlayer interactions in the ab-planes. We argue that it should not lead to weak ferromagnetism of neither conventional nor hidden type. Instead, the distribution of Dzyaloshinskii–Moriya vectors is typical for helimagnets. However, the occurrence of helimagnetism appears unlikely due to the assumed hierarchy of the magnitudes of spin interactions and the opposite chirality in adjacent ab-planes.

DOI: 10.12693/APhysPolA.137.945

PACS/topics: magnetic anisotropy, Dzyaloshinskii–Moriya interaction, collinear Néel order

1. Introduction

$Cu(en)(H_2O)_2SO_4$ (en = $C_2H_8N_2$) (CUEN) was originally identified as a quasi-two-dimensional (2D) easy-plane Heisenberg antiferromagnet (HAF) with spin $S = 1/2$ on the spatially anisotropic triangular lattice [1], which becomes magnetically ordered below $T_N = 0.91$ K. Recent experimental and theoretical study established CUEN as a representative of the $S = 1/2$ HAF on a zigzag square lattice [2] within the magnetic bc-layers. This picture, suggested by *ab-initio* calculations [3], was corroborated by finite-temperature quantum Monte-Carlo simulations and single-crystal measurements of the specific heat, susceptibility, and magnetization. Symmetry analysis of magnetic layers indicated only the presence of symmetric spin exchange anisotropies (SEA) and anticipated an easy-axis within the easy plane. The easy-axis was identified experimentally through the observation of a spin-flop transition in a magnetic field 200 mT applied along the b-axis.

The emerging picture of a collinear HAF with two intralayer SEA is mostly consistent with the data, but some issues remain unexplained. More specifically, the differences in the susceptibility measured in the field-cooling and zero-field-cooling regimes, the susceptibility peak below the Néel temperature [2], and the observed hysteresis in a field along the b-axis [4] suggest the presence of hidden spin canting of unknown origin. On the other hand, such canting is usually produced by antisymmetric Dzyaloshinskii–Moriya [5, 6] spin interactions (DMI), which are allowed for the interlayer couplings [1]. The study of the interlayer interactions is accentuated by the recent antiferromagnetic-resonance (AFMR) experiments on CUEN [7] which confirmed the existence of the two $q = 0$ magnon gaps, but also observed a small splitting of both branches. Invoking a small isotropic interlayer coupling [8] could explain the splitting, but not its actual observation in a collinear antiferromagnet (AF), because the two of the eigenmodes do not couple to the rf-field and should not be excited.

Our goal is to analyse interlayer spin interaction in CUEN and elucidate the role of the individual terms. We argue that the DMI in CUEN should not lead to the spin canting, and emphasize the need for an alternative explanation of the experiment.

2. Crystal symmetry and the intralayer spin interactions

CUEN crystallizes in the monoclinic symmetry with the space group $C2/c$ which is preserved at least down to 0.4 K [1]. The room-temperature lattice parameters are $a = 7.23$ Å, $b = 11.73$ Å, $c = 9.77$ Å, $\beta = 105.5°$, and $Z = 4$ [9]. The four translationally inequivalent Cu atoms within the unit cell are denoted as A, B, C, and D. In the following, the spins $S = 1/2$ located on the Cu atoms are denoted by their standard symbol $\boldsymbol{S}$, or by $\boldsymbol{A}$, $\boldsymbol{B}$, $\boldsymbol{C}$, $\boldsymbol{D}$

*corresponding author; e-mail: alzbeta.orendacova@upjs.sk

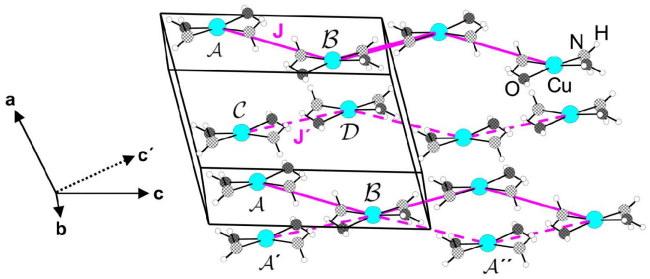

Fig. 1. Crystal structure of CUEN. The four translationally inequivalent Cu atoms within the unit cell are denoted as A, B, C, and D. The axis $c\prime$ lies in the ac-plane and is orthogonal to a and b axes. The two major (antiferromagnetic) exchange interactions found by *ab initio* studies [3], J and J', lie in the bc-layers. (Reproduced with permission from Ref. [2]).

when a distinction between the four sublattices becomes necessary. The major spin interactions suggested by *ab-initio* studies [3] occur within the basal ($\boldsymbol{A}$, $\boldsymbol{B}$ spins) and middle bc-layers ($\boldsymbol{C}$, $\boldsymbol{D}$ spins) where the symmetry precludes the existence of DMI [2] (Fig. 1).

The isotropic exchange interaction between the nearest neighbors within the bc-layer takes J and J' values, whereas the SEA is described by four (symmetric) matrices. Assuming the spins to be spatially uniform on each sublattice, most of the off-diagonal elements average out to zero. The rest can be diagonalized by a suitable rotation around the b-axis [2]. This rotation defines the new orthogonal axes 1, 2, 3, with $2 \parallel b$.

Interestingly, the axes 1 and 3 nearly coincide with the a and c' axes. Within the mean field theory, the only effective parameters are the isotropic exchange $\tilde{J} = \frac{1}{2}(J + J')$, and the in-plane $\tilde{G}_{\rm in}$ and out-of-plane $\tilde{G}_{\rm out}$ anisotropies. The energy per spin in a magnetic field $\boldsymbol{H}$ is then given as

$$W_S = \tilde{J}\boldsymbol{A}\cdot\boldsymbol{B} - \frac{1}{2}g\mu_{\rm B}\boldsymbol{H}(\boldsymbol{A}+\boldsymbol{B}) - \tilde{G}_{\rm in}A_3B_3 - \tilde{G}_{\rm out}A_1B_1, \quad (1)$$

where g is the usual g-factor, $\tilde{J} > 0$, and $\mu_{\rm B}$ is the Bohr magneton. The components of $\boldsymbol{A}$ ($\boldsymbol{B}$) spins along the axes 1, 3, respectively, are denoted as A_1 and A_3 (B_1 and B_3), respectively. Consistency with the experiment requires $\tilde{G}_{\rm out} > \tilde{G}_{\rm in} > 0$. The values $\tilde{G}_{\rm in}$, $\tilde{G}_{\rm out}$ ($\approx 10^{-3}\tilde{J}$) are directly related to the $q = 0$ magnon gaps [2, 7]. Spin interactions in the middle bc-layers are completely isomorphic. The corresponding energy is obtained from (1) by $\boldsymbol{A} \to \boldsymbol{C}$, $\boldsymbol{B} \to \boldsymbol{D}$. For $\boldsymbol{H} = 0$, above equation is minimized by the collinear spins $\boldsymbol{A}$, $\boldsymbol{B}$. Even more transparent formulation of (1) can be obtained in terms of the "uniform magnetization" $\boldsymbol{m} = (\boldsymbol{A}+\boldsymbol{B})/(2s)$, and the "staggered magnetization" $\boldsymbol{n} = (\boldsymbol{A}-\boldsymbol{B})/(2s)$. If $g\mu_{\rm B}Hs \ll \tilde{J}$, weak anisotropies imply $|\boldsymbol{m}| \ll |\boldsymbol{n}|$. Here, $\boldsymbol{m}$ can be treated as small quantity of order ε. Then, to leading order, $\boldsymbol{m}\cdot\boldsymbol{n} = 0$, $\boldsymbol{n}^2 = 1$. It is useful to introduce rescaled (dimensionless) parameters $g_{\rm in} = 2\tilde{G}_{\rm in}/\varepsilon^2\tilde{J}$, $g_{\rm out} = 2\tilde{G}_{\rm out}/\varepsilon^2\tilde{J}$, and magnetic field parameter $\boldsymbol{h} = g\mu_{\rm B}\boldsymbol{H}/(2s\varepsilon\tilde{J})$, which are all of the order of unity. Then, the rescaled energy per spin w_S (in units of $s^2\varepsilon^2\tilde{J}$), and $\boldsymbol{m}$ can be expressed entirely in terms of $\boldsymbol{n}$, namely

$$w_S = \left[g_{\rm out}n_1^2 + g_{\rm in}n_3^2 + (\boldsymbol{n}\cdot\boldsymbol{h})^2\right]/2,$$
$$\boldsymbol{m} = -\frac{\varepsilon}{2}\left[\boldsymbol{n}\times(\boldsymbol{n}\times\boldsymbol{h})\right]. \quad (2)$$

The energy of the pure Néel state is removed from (2). One may fix ε by, e.g. setting $g_{\rm in} = 1$, which in turn sets the (rescaled) spin-flop field $h_{SF} = 1$. At $\boldsymbol{h} = 0$, w_S is minimized by $n_2 = \pm 1$ and $\boldsymbol{m} = 0$. This indicates the lack of intrinsic spin canting mechanism within the bc-layers.

3. Interlayer interactions

3.1. Interlayer couplings along the ab-planes

We now discuss the interlayer interactions between the nearest neighbors (NN) within the ab-planes, (i.e., the spin pairs $\boldsymbol{A}$, $\boldsymbol{C}$, and $\boldsymbol{B}$, $\boldsymbol{D}$ in Fig. 2). We assume the modification of the 2D interactions introduced in Sect. 2 to be of the form

$$W_\perp = \sum_{\langle\langle kl\rangle\rangle}\left[J_{kl}\,(\boldsymbol{S}_k\cdot\boldsymbol{S}_l) + \boldsymbol{D}_{kl}\cdot(\boldsymbol{S}_k\times\boldsymbol{S}_l) + \sum_{i,j}K_{kl}^{ij}\left(S_k^iS_l^j + S_l^iS_k^j\right)\right], \quad (3)$$

where $\langle\langle kl\rangle\rangle$ is an interlayer NN spin pair. We state our results in the aforementioned coordinate frame 1, 2, 3 of Sect. 2. The isotropic exchange takes a single value $J_{kl} = J_\perp$ for all NN neighbors in the ab-planes. The SEA is described by two symmetric matrices K_I and K_{II}, whose distribution over the lattice is shown in Fig. 2:

$$K_I = \begin{pmatrix} K_{11} & K_{12} & K_{13} \\ K_{12} & K_{22} & K_{23} \\ K_{13} & K_{23} & K_{33} \end{pmatrix},$$

$$K_{II} = \begin{pmatrix} K_{11} & -K_{12} & K_{13} \\ -K_{12} & K_{22} & -K_{23} \\ K_{13} & -K_{23} & K_{33} \end{pmatrix}. \quad (4)$$

Finally, DMI are indeed present, as anticipated in [1], and are restricted to the two vectors, see Fig. 2:

$$\boldsymbol{D}_I = (D_1, D_2, D_3),$$
$$\boldsymbol{D}_{II} = (D_1, -D_2, D_3). \quad (5)$$

Note that the sign of the DMI vectors is opposite for the $\boldsymbol{A}$, $\boldsymbol{C}$, and $\boldsymbol{B}$, $\boldsymbol{D}$ spins.

The isotropic exchange contributes to the total energy as $J_\perp\,(\mathbf{A}\cdot\mathbf{C} + \mathbf{B}\cdot\mathbf{D})$. Using the interlayer staggered magnetization defined in Sect. 2, this contribution can be, to leading order, rewritten as $J_\perp(n_L\cdot n_U)$.

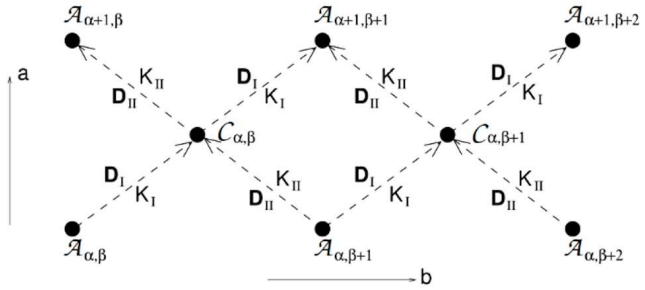

Fig. 2. Distribution of the DMI vectors and the SEA matrices on a portion of the *ab*-plane. The arrows indicate the order of spins in the cross product of (3). The indices α, β advance along the crystal axes a, b. The index γ along the axis c is identical for all displayed spins and is omitted. Spin interactions between the spins $\boldsymbol{B}$, $\boldsymbol{D}$ may be obtained by replacing in this figure the sublattice symbols $A \to B$, $C \to D$, and simultaneously reversing the sign of all DMI vectors $\boldsymbol{D}_I \to -\boldsymbol{D}_I$, $\boldsymbol{D}_{II} \to -\boldsymbol{D}_{II}$.

The subscripts L and U distinguish between the intralayer staggered magnetizations in the basal and the middle *bc*-planes. $J_\perp$ is expected to be of the order of the intralayer SEA [8]. Its role at low-temperatures is mainly to affect the mutual spin orientations (chooses between parallel/antiparallel order) in the adjacent *bc*-layers, and does not lead to the departure from the collinear order. The same holds for the diagonal contribution of the interlayer SEA of (4). Concerning the off-diagonal SEA, K_{12}, K_{23} are within the mean-field theory averaged out to zero. In principle K_{13} can also be eliminated by diagonalization as in Sect. 2, however both the intralayer and the interlayer off-diagonals cannot be eliminated simultaneously. Its contribution reduces to $K_{13}\,(A_1C_3 + A_3C_1 + B_1D_3 + B_3D_1)$ or, to leading order, $K_{13}\,(n_{L1}n_{U3} + n_{L3}n_{L1})$. It does not appear to produce spin canting at zero field. In particular, it does not couple to the component along the axis 2. The ground state certainly comprises of sizable component along this axis.

Concerning the DMI, the inspection of Fig. 2 makes it clear that, for the spins uniform on each sublattice, the DMI contribution is actually zero, with no weak-ferromagnetism. This is also supported by the fact that weak ferromagnetism requires the DMI vector to alternate in sign on opposite bonds [10]. The lack of such alternation indicates a possible occurrence of helimagnetism — the collective rotation of spins, but it is unlikely to occur when $J_\perp \ll \tilde{J}$. The chirality (the sign of the DMI) for $\boldsymbol{A}$, $\boldsymbol{C}$ and $\boldsymbol{B}$, $\boldsymbol{D}$ spins is opposite. They are set to rotate in opposite sense. Then the mutual orientation of, say, $\boldsymbol{A}$ and $\boldsymbol{B}$ would necessarily vary throughout the lattice. In contrast, strong $\tilde{J}$ requires that $\boldsymbol{A}$ and $\boldsymbol{B}$ remain nearly antiparallel all the time. Incommensurate magnetism could in principle occur if $\tilde{J} \ll J_\perp$. Then the DMI is comparable to $\tilde{J}$, being strong enough to overcome energetically unfavorable configurations [11].

3.2. Interlayer couplings along the ac-planes

We have also examined the interactions between the nearest and the next-nearest neighbors along the *ac*-planes. Our symmetry analysis revealed that only symmetric exchange anisotropies are present, and DMI is precluded by symmetry. However, the structure of SEA is similar to those already explicitly presented, and does not bring in any new qualitative elements.

4. Conclusions

We have studied the interlayer spin interactions in the antiferromagnet CUEN. We have confirmed the presence of antisymmetric interlayer exchange interactions, and examined them in detail. We found that the Dzyaloshinskii–Moriya interactions do not lead to weak-ferromagnetism of any type. Instead, they admit the existence of helimagnetism, whose actual occurrence, however, is not favored by the system parameters. Similarly, the structure of symmetric exchange interactions does not indicate any obvious spin canting mechanism. The explanation of the experimental results thus requires additional effort.

Acknowledgments

This work was supported by projects VEGA 1/0269/17, APVV-14-0073, APVV-18-0197, APVV-14-0078, VVGS-PF-2018-787, and Path to Exascale project No. CZ.02.1.01/0.0/0.0/16_01 3/0001791.

References

[1] R. Tarasenko, A. Orendáčová, E. Čižmár, et al., *Phys. Rev. B* **87**, 174401 (2013).

[2] L. Lederová, A. Orendáčová, J. Chovan, et al., *Phys. Rev. B* **95**, 054436 (2017).

[3] R. Sýkora, D. Legut, *J. Appl. Phys.* **115**, 17B305 (2014).

[4] L. Lederová, A. Orendáčová, R. Tarasenko, J. Chovan, M. Mihálik, M. Orendáč, A. Feher, "Weak Ferromagnetism in the Two-Dimensional Monoclinic Quantum Magnet $Cu(en)(H_2O)_2SO_4$", in preparation.

[5] I. Dzyaloshinskii, *Phys. Chem. Solids* **4**, 241 (1958).

[6] T. Moriya, *Phys. Rev.* **120**, 91 (1960).

[7] V.N. Glazkov, Yu.V. Krasnikova, I.K. Rodygina, J. Chovan, R. Tarasenko, A. Orendáčová, *Phys. Rev. B* **101**, 014414 (2020).

[8] J. Chovan, N. Papanicolaou, *Eur. Phys. J. B* **17**, 581 (2000).

[9] V. Manríqez, M. Campos-Valette, N. Lara, N. González-Tejeda, O. Wittke, G. Díaz, S. Diez, R. Muñoz, L. Kriskovic, *J. Chem. Crystallogr.* **26**, 15 (1996).

[10] N. Papanicolaou, *Phys. Rev. B* **55**, 12290 (1997).

[11] J. Chovan, M. Marder, N. Papanicolaou, *Phys. Rev. B* **88**, 064421 (2013).